Towards continuous long-term measurements of suspended particulate matter (SPM) in turbid coastal waters

**Thomas H. Badewien · Elke Zimmer ·
Alexander Bartholomä · Rainer Reuter**

Abstract The dynamics of sediment transport in the
East Frisian Wadden Sea are important for the coastal
zone and for ecosystem functioning. The tidal inlets be-
tween the East Frisian islands connect the back-barrier
intertidal flats to the North Sea. Here, concentrations
of suspended particulate matter (SPM) in the water
column are highly variable, depending on weather con-
ditions and tides. In order to estimate the nature and
quantity of sediment transport, in situ measurements
were carried out at a Time Series Station in the tidal
inlet between the islands of Spiekeroog and Langeoog.
This study shows the suitability of multispectral trans-
missometry (MST) for obtaining long-term SPM mea-
surements with high resolution. The comparability of
this technique to the standard filter method and the
laser diffraction method [laser in situ scattering and
transmissometry (LISST)] is demonstrated. In addition,
the Junge coefficients derived from both MST and
LISST measurements are compared. A time series of
SPM data covering nearly 4 months is presented. As a
major result, the data reveal that a single storm surge
can have less impact on SPM dynamics than longer-
lasting gales. This high-resolution long-term data set is
very valuable for modelling suspended matter flux. It
also provides background information for studying the
influence of SPM dynamics on coastal sediments.

Keywords Wadden Sea · SPM measurements ·
Time series data · Storm surge · Multispectral
transmissometer · Junge coefficient

T. H. Badewien (✉) · E. Zimmer · R. Reuter
Institute of Physics, University of Oldenburg,
Carl-von-Ossietzky-Str. 9-11, 26129 Oldenburg, Germany
e-mail: thomas.badewien@uni-oldenburg.de

A. Bartholomä
Senckenberg Institute, Südstrand 40, 26382 Wilhelmshaven,
Germany

1 Introduction

The dynamics of suspended particulate matter (SPM)
are important for the coastal zone and ecosystem
functioning of the East Frisian Wadden Sea (German
Bight). These dynamics govern processes such as sedi-
ment transport and primary production, the latter being
limited by light availability in the water column. The
Wadden Sea is characterised by high tidal forcing from
the North Sea (Santamarina and Flemming 2000), and
extreme storm events have a profound influence on the
sediment budget (Lumborg and Pejrup 2005).

The tidal inlets between the East Frisian Islands con-
nect the processes on the intertidal flats to the forcings
from the North Sea. Here, current velocities rise up
to 1.6 ms^{-1} (Reuter et al. 2009; Puncken et al. 2006),
leading to a high transport of SPM. In order to obtain
full understanding of the complex dynamics, SPM con-
centrations have to be measured on different temporal
and spatial scales. Satellite imagery can resolve concen-
trations of SPM on a large spatial scale but is confined
to surface data. Also, clear weather conditions have to
coincide with high water, which limits the availability
of suitable satellite observations (Gemein et al. 2006;
Astoreca et al. 2006). Another option is airborne dig-
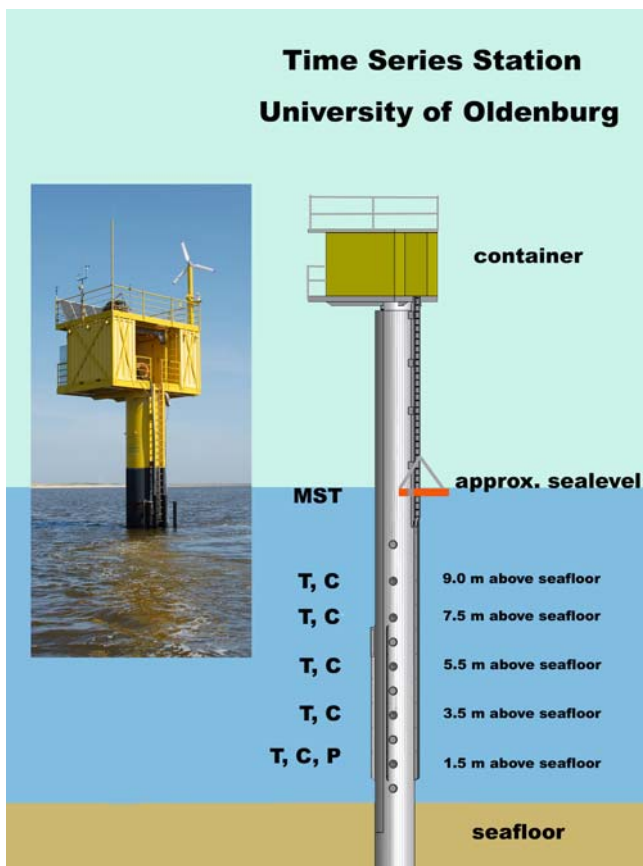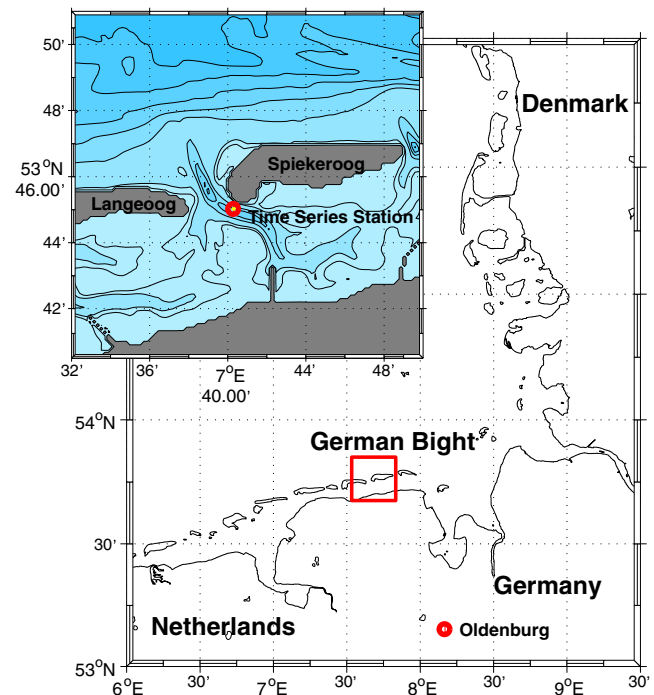ital imaging, which provides high-resolution data on a

Fig. 1 Schematic representation of the Time Series Station. *Symbols* depict the sensor levels in the water column. T = temperature, C = conductivity, P = pressure, MST = multispectral transmissometer. *Photo* shows the station at nearly high-water level

Fig. 2 Research area: German Bight, Wadden Sea. The *inset* shows the position of the Time Series Station in the tidal inlet between the islands of Langeoog and Spiekeroog

spatial scale of approximately 20 cm (Mehrtens et al. 2009). However, both methods have to be combined with measurements providing high temporal resolution. Since shipboard observations are limited in time and, therefore, often miss extreme events when optical remote sensing data are typically unavailable, continuous in situ measurements are essential.

At the Wadden Sea Time Series Station (Fig. 1), which is located in the tidal inlet between the islands of Spiekeroog and Langeoog (Fig. 2), continuous hydrographic measurements have been carried out since autumn 2002. Details of the Time Series Station can be found in Reuter et al. (2009). This Time Series Station is an excellent platform for obtaining SPM long-term data irrespective of weather conditions.

Different optical and acoustical methods can be used for estimating SPM concentrations in situ with high temporal resolution; see, for example, Winter et al. (2007). An option is the use of a multispectral transmissometer (MST), a method which was developed

and applied by Barth et al. (1997). In contrast to monochromatic instruments, the multispectral method is capable of distinguishing different substances, such as Gelbstoff, phytoplankton and SPM, contributing to light attenuation in natural waters. This is particularly valuable in coastal waters such as the Wadden Sea, which has high concentrations of Gelbstoff from terrestrial sources. Barth et al. (2000) showed the suitability of the multispectral technique for short-term (several hours), shipboard measurements in estuaries and the North Sea.

This study was conducted to demonstrate that MST can also be applied to obtain long-term, high-resolution SPM data. Therefore, a MST was installed at the Time Series Station in the tidal inlet in autumn 2006. For this purpose, the algorithms for evaluating the data had to be adapted for the use in the Wadden Sea (see Section 2). Additionally, in order to ensure the method's quality, MST-derived SPM data were compared both to SPM concentrations obtained by the standard filter method and to laser in situ scattering and transmissometry (LISST) during shipboard experiments. In addition, MST-data were calibrated and validated by laboratory and in situ measurements. Time series data obtained during winter 2007/2008 are presented and discussed, highlighting the importance of

continuous measurements to observe extreme events such as storm surges.

2 Methods

2.1 Instruments

2.1.1 Multispectral transmissometer

The MST measures beam attenuation coefficients in the visible wavelength range from 340 to 785 nm. It consists of a cylindrical probe housing (470 mm long, 110 mm in diameter) with two optical windows at the bottom and a triple-prism retroreflector, which is set at distances between near zero and 200 mm from the windows (Figs. 3 and 4). This enables the optical pathlength to be as much as 400 mm. A flash lamp emits a near-parallel light beam with high emission intensity between the near ultraviolet and the far red. A beam splitter produces collimated beams for the sample and reference signal that are detected at the same time. The beam divergence angle and the beam acceptance angle are both 0.57 °. These angles are critical since large particles exhibit strong small-angle forward scattering, which must be rejected from the detected signal to retrieve the true attenuation coefficient c for parallel light. According to Austin and Petzold (1977), using the angle mentioned above for measurements in coastal waters results in an error less than 10%.

The variable pathlength of the MST offers the possibility to adapt to different turbidity conditions and, thus, to optimise the signal-to-noise ratio of the measurements. This feature is also used for calibrating the device: The reflector is moved as close as possible to the optical window until almost no water is left in the gap. The resulting measurements are used to correct for instrument-specific changes in situ before and after each measuring period. This cannot be achieved by using static-pathlength transmissometers. For further details, see Barth et al. (1997) and Barth et al. (2000).
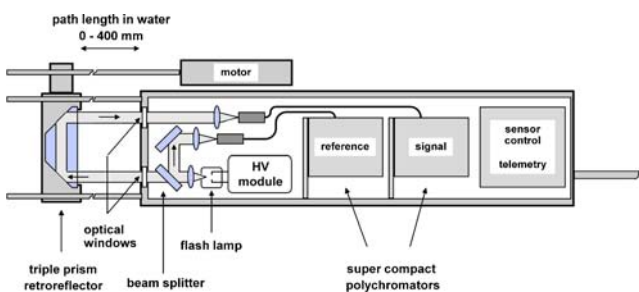
Fig. 3 Schematic representation of the MST
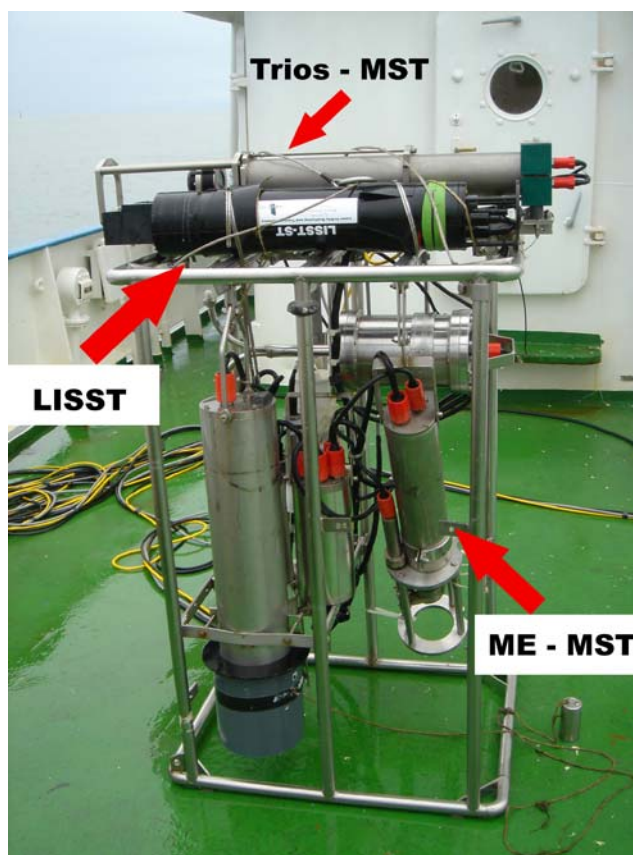
Fig. 4 Photo of instrument setup during research cruise aboard *FK Senckenberg* in October 2007. CTD, ME-MST, Trios-MST and LISST were mounted to the same frame in order to ensure comparability of measurements

The attenuation coefficient c is calculated via algorithms that are based on the loss of light intensity I over the path length x (Lambert's law $dI/I = -c \, dx$) and is composed of several terms of absorption and scattering by molecules and particles,

$$c(\lambda) = c_w(\lambda) + c_{pp}(\lambda) + c_{tp}(\lambda) + a_d(\lambda) \quad (m^{-1}), \qquad (1)$$

where the indices refer to contributions from water (w), phytoplankton (pp) and transparent particles (tp). The scattering of Gelbstoff is insignificant; therefore, only the Gelbstoff absorption coefficient (a_d) is needed. The attenuation coefficient of water (c_w) is nearly independent of salinity and temperature over the spectral range from 370 to 700 nm. Therefore, the spectrum of purified water is subtracted from Eq. 1.

$$c(\lambda) - c_w(\lambda) = \alpha c_{pp}^*(\lambda) + \beta c_{tp}^*(\lambda) + \gamma a_d^*(\lambda) \quad (m^{-1})$$

$$(2)$$

The asterisk terms are dimensionless spectral functions related to the specific substances. The factors

(α), (β) and (γ) represent the relative contributions of the individual substances to the entire spectrum and, therefore, the substance concentration. Based on a few assumptions, algorithms to calculate these factors were established by Barth et al. (1997):

Transparent particles The term "transparent particles" includes various kinds of hydrosols with low and spectrally unspecific absorption characteristics, having a size distribution from less than 100 nm to the millimetre range. This size range is optically effective due to their scattering behaviour and may contribute to the attenuation of light. With the size distribution function for the particle number vs particle radius

$$n_{tp}(r) = \frac{\mathrm{d}N_{tp}}{\mathrm{d}r} \tag{3}$$

and using a normalised particle radius $\rho = r/r_0$, with (r) the particle radius and (r_0) an arbitrary reference radius, the optically effective size range may be described by Junge's law for a hyperbolic size distribution:

$$n_{tp}(\rho) = s\rho^{-c_j} \tag{4}$$

(N_{tp}) constitutes the total number of particles per unit volume, (c_j) is the Junge coefficient, and (s) a concentration-dependent parameter. Usually, (c_j) ranges between approximately 3 and 5. Then, the attenuation coefficient for the transparent particles is given by:

$$c_{tp}^*(\lambda) = \lambda^{(3-c_j)} \tag{5}$$

For details, see Reuter (1980) and Diehl and Haardt (1980).

Gelbstoff Gelbstoff consists of dissolved organic molecules of natural origin with a broad spectrum of molecule sizes. To approximate, the absorption coefficient (a_d) can be assumed as an exponential function, with a virtually constant parameter s in the range from 300 to 600 nm. (a_d) is normalised to unity at (λ_0) = 357 nm:

$$a_d^*(\lambda) = e^{[-s(\lambda - \lambda_0)]} \tag{6}$$

gives a good approximation for the Gelbstoff absorption coefficient (a_d) (Bricaud et al. 1981).

Phytoplankton For the purpose of this study, the factor α in Eq. 2 for phytoplankton *pp* was set to zero, assuming that the primary producers are absent during winter months.

Fitting routine In order to obtain the parameters in Eq. 2 from a measured spectrum, a Monte Carlo routine using a similarity analysis has to find the optimum parameter set that minimises the deviation between a measured and a reconstructed spectrum by searching for the minimum of the deviation function:

$$D = \left\| [c(\lambda) - c_w(\lambda)] - \alpha c_{pp}^*(\lambda) - \beta c_{tp}^*(\lambda) - \gamma a_d^*(\lambda) \right\| \tag{7}$$

Two similarly constructed MST instruments from different manufacturers were used: ME-MST (Meerestechnik-Elektronik GmbH, Trappenkamp, Germany; now: ME Grisard GmbH, Kiel, Germany) and Trios-MST (TriOS Optical Sensors GmbH, Oldenburg, Germany). These devices differ slightly in their optical design and performance.

2.1.2 Laser in situ scattering and transmissometry

In this study, a laser in situ scattering and transmission meter (LISST-100 type C, Sequoia Scientific, Bellevue, WA, USA) was used. The instrument has an overall length of 810 mm and a diameter of 130 mm (Fig. 4). It measures the particle size distribution of suspended material, as well as optical transmission, temperature and pressure. Particle scattering is detected at 32 angles, and this information is solved for 32 unknowns, which gives the particle volume concentration in 32 size classes over a logarithmic radius scale $\mathrm{d}V(\rho)/\mathrm{d}ln(\rho)$, with $\mathrm{d}ln\rho = 0.166$ and ρ being the normalised particle radius. With the relation $\mathrm{d}\rho = \rho\mathrm{d}ln\rho$, this can be transformed to the size distribution function of particle volume vs particle radius:

$$v(\rho) = \frac{\mathrm{d}V(\rho)}{\mathrm{d}\rho} = \frac{1}{\rho}\frac{\mathrm{d}V\rho}{\mathrm{d}ln\rho} \tag{8}$$

The relation with the number distribution function, Eq. 3, is:

$$v(\rho) = \frac{4\pi}{3}\rho^3 n(\rho) \tag{9}$$

Assuming Junge's hyperbolic size distribution function, Eq. 4, it follows:

$$v(\rho) = \frac{4\pi}{3}s\rho^{3-c_j} \tag{10}$$

This corresponds to LISST particle volume data in the form:

$$\frac{\mathrm{d}V(\rho)}{\mathrm{d}ln\rho} = \frac{4\pi}{3}s\rho^{4-c_j} \tag{11}$$

A forward scattering analysis is conducted, assuming the laser light diffraction by spherical particles at small forward scattering angles is approximately identical to the diffraction by an aperture of equal size.

The effect of refractive index of particles is negligible to the distribution of light scattering at small forward angles. The LISST-100 uses a series of 32 annular logarithmically scaled detectors that measure the forward-scattered laser light intensity distribution through a 50-mm laser path length. In this study, the path length was reduced because of the high turbidity of the water in the study area.

The range of the diffraction angles determines the observable size range of the scatterers (2.5 to 500 μm). The error of the measurement is within a range of 10% and increases with increasing particle size class. For further details, see Agrawal and Pottsmith (2000), Agrawal (2005) and Agrawal et al. (2008).

2.1.3 Filter method

Water samples were taken by bucket at 0.5–1 m depth and filtered onto precombusted (450°C, 6 h) and preweighed GF/F filters (Whatman Schleicher and Schüll, 47 mm diameter and pore size of 0.7 μm). Filters were rinsed with distilled water and stored frozen (−20°C) until drying for 12 h at 60°C in the laboratory. The filters were reweighed for determination of SPM. The weight was related to the volume of the filtered water and normalised to 1 l.

2.2 Experiments

2.2.1 Laboratory

In order to assess whether the algorithms used for MST measurements is suitable for estimating inorganic particles, the following tank experiment was carried out. The ME-MST and the Trios-MST were deployed in a tank filled with 80 l seawater. Sediment from the Wadden Sea was baked at 450°C for 6 h to remove organic substances and added at six different concentrations to the water in the tank. A commercially available in situ water pump was used for maintaining a homogeneous distribution of particles. At each concentration, the MST measurements were taken for 10 min and a mean value was calculated. Simultaneously, two to three filter samples were taken in the middle of the measuring period. Filter samples were treated as described above.

2.2.2 Shipboard measurements

In situ measurements were conducted during two cruises with *FK Senckenberg* in the East Frisian Wadden Sea in October 2007 and February 2008. The sampling site is located in the tidal inlet of the back-barrier area of the island Spiekeroog (Otzumer Balje

53° 44.87′ N and 7° 40.30′ E). On 17 October 2007, data were collected over a tidal cycle from high tide to high tide. Depth profiles of temperature and conductivity were measured by a conductivity–temperature–depth (CTD) probe (OTS 3000 Meerestechnik-Elektronik GmbH, Germany) along with ME-MST, Trios-MST and LISST measurements in intervals of 30 min over the sampling period. The instruments were mounted to the same frame in order to ensure measurement comparability (Fig. 4). Every second profile, samples for filtration were collected from the sea surface by bucket. On 26 February 2008, depth profiles were measured by CTD and ME-MST from low tide to low tide, again at intervals of 30 min, and samples for filtration were collected as above during each of these profiles.

2.2.3 Time Series Station

For continuous measurements, the Trios-MST was mounted to the Time Series Station (Fig. 1) in the Wadden Sea, located at 53° 45.02′ N and 7° 40.27′ E (Reuter et al. 2009). The data presented were obtained from 22 October 2007 to 13 February 2008. The measuring interval is 4 min. The measuring depth is about 3 m at high water and close to the sea surface at low water due to the MST's fixed position at the station. At extreme low water levels, the instrument sticks out of the water. These data are discarded.

On workdays, the MST is calibrated by remote control: The reflector is moved as close as possible to the optical window until almost no water is left in the gap. This position is held for at least 30 min and data are taken every 4 min. The resulting measurements are used to correct for instrument-specific changes such as flashlamp degradation or growth of biofilms on the optical surfaces. This is also a useful tool for service personnel to decide whether a mechanical cleaning is necessary. Biofouling of optical windows is indeed a limiting factor of these long-term measurements. However, it turned out that effects from biofilms can be well compensated with the self-calibration using the moving retroreflector and the procedure described above. Usually, maintenance has to be carried out every 2 to 3 weeks during summer.

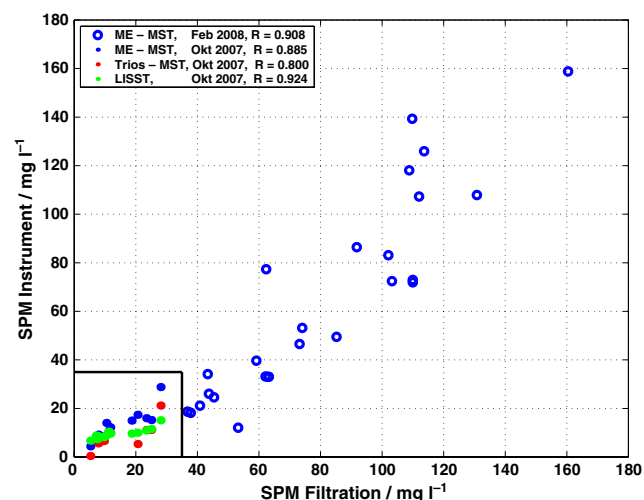## 3 Results

3.1 Comparison of methods

MST measurements were compared to filter-based data in laboratory and shipboard experiments in order to analyse the suitability of the former method to estimate
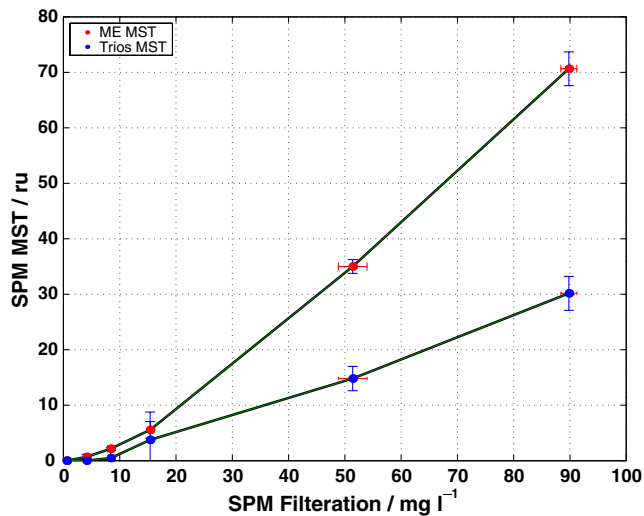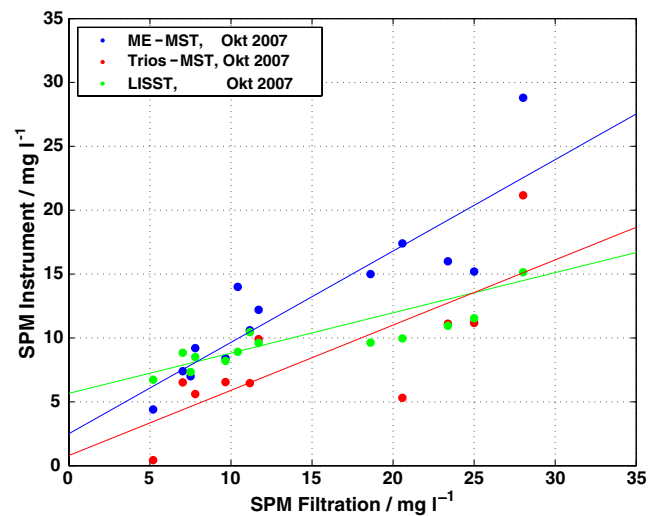
Fig. 5 Laboratory experiment: SPM concentrations obtained by the filter method vs relative MST data

Fig. 7 Surface SPM data obtained by the filter method correlated to ME-MST-, Trios-MST- and LISST-derived data during the research cruise in October 2007

SPM concentrations in seawater. MST-derived values correspond well with SPM data obtained from the filter method under laboratory conditions (Fig. 5). The strong relationship indicates the suitability of the MST to estimate SPM. The variation in slope results from instrument-specific differences such as the adjustment of the optical elements. Here, the light beam divergence and the detector reception angle of incidence play a crucial role, especially in highly turbid waters (Austin and Petzold 1977).

To further scrutinise whether MST measurements are comparable to established methods for estimating SPM in turbid coastal waters, shipboard measurements

were conducted in October 2007 and February 2008. These data also indicate a linear relationship between SPM data obtained by MST or LISST and by the filter method (Figs. 6 and 7). Correlation coefficients are $R = 0.885$ ($n = 13$), $R = 0.800$ ($n = 11$) and $R = 0.924$ ($n = 13$) for data obtained in October 2007 by the ME-MST, Trios-MST and LISST, respectively. MST and LISST values correspond well with each other. In February 2008, SPM values were up to ten times higher than those in October 2007. Still, filter-based measurements and ME-MST data correlate well ($R = 0.908$, $n = 25$).

In order to evaluate whether the particle size distribution in the study area follows Junge's law, the
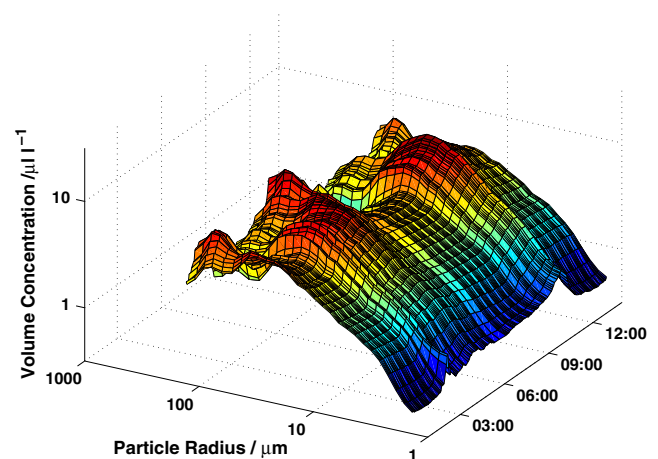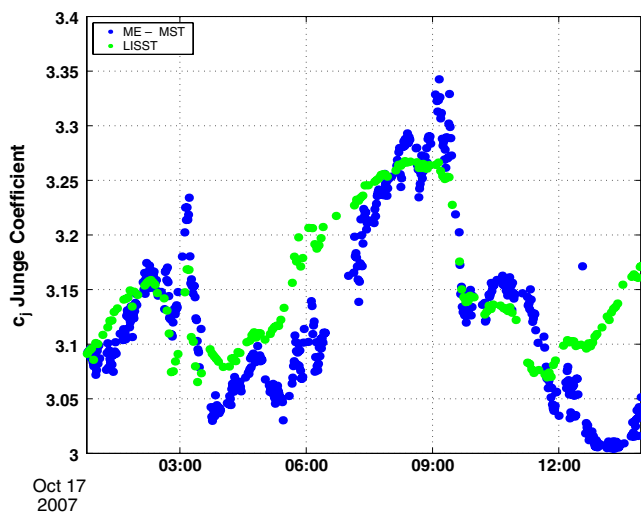

Fig. 6 Surface SPM data obtained by the filter method correlated to ME-MST-, Trios-MST- and LISST-derived data during two research cruises
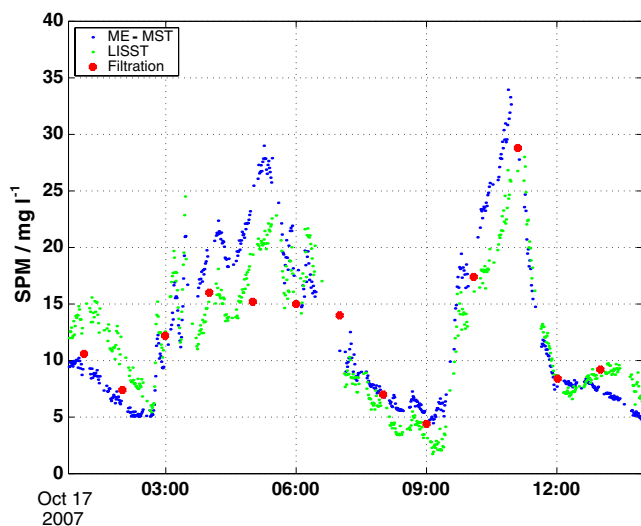

Fig. 8 Double logarithmic plot of particle volume concentration vs particle radius derived from LISST data. Time series from the sea surface during the research cruise on 17 October 2007
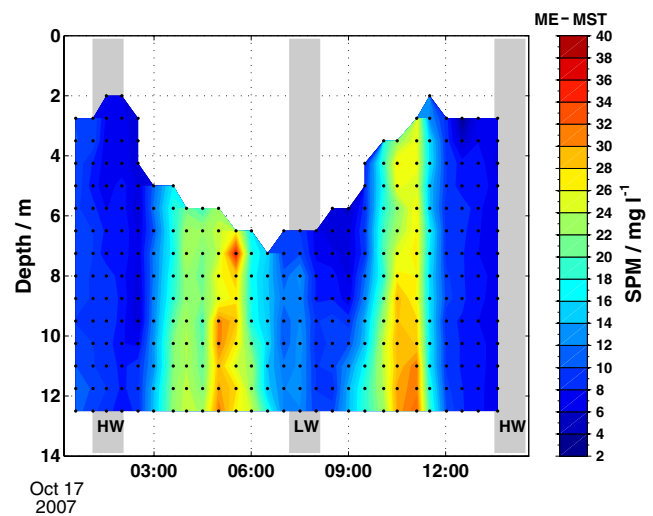
Fig. 9 Time series of Junge coefficient derived from ME-MST and LISST measurements at the sea surface during the research cruise on 17 October 2007

Fig. 11 SPM measured with ME-MST by vertical profiling and gridded to 0.75 m intervals (October 2007). Data are related to the seafloor. *HW*: high water, *LW*: low water

particle volume concentration vs particle radius derived from LISST data in October 2007 were plotted on logarithmic scales (Fig. 8). In the particle size range with radiuses from 1.25 to 26.9 μm, this relationship is indeed linear, with the slope corresponding to the Junge coefficient. The distribution of this parameter is shown in Fig. 9, green dots. This plot also shows that LISST- and MST-derived Junge coefficients follow the same pattern. The values are rather low, ranging from 3 to 3.35. If the Junge coefficient has small values, large particles dominate.

In Fig. 10, the surface SPM data obtained during the October 2007 cruise are shown as time series. This demonstrates that ME-MST-, LISST- and filter-derived data show similar patterns and concentrations, thus indicating the comparability of the methods. However, the filter method clearly misses pronounced peaks in this highly dynamic system due to undersampling. This is overcome by the continuous measurements.

The contour plots of the data derived from the depth profiles of ME-MST and LISST measurements illustrate the vertical variability of SPM concentrations
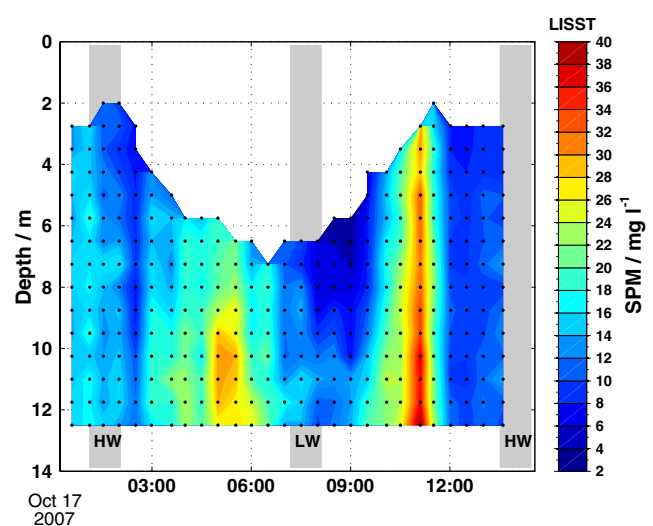

Fig. 10 Time series data of SPM concentrations measured with ME-MST, LISST and filter method of samples taken at the sea surface in October 2007
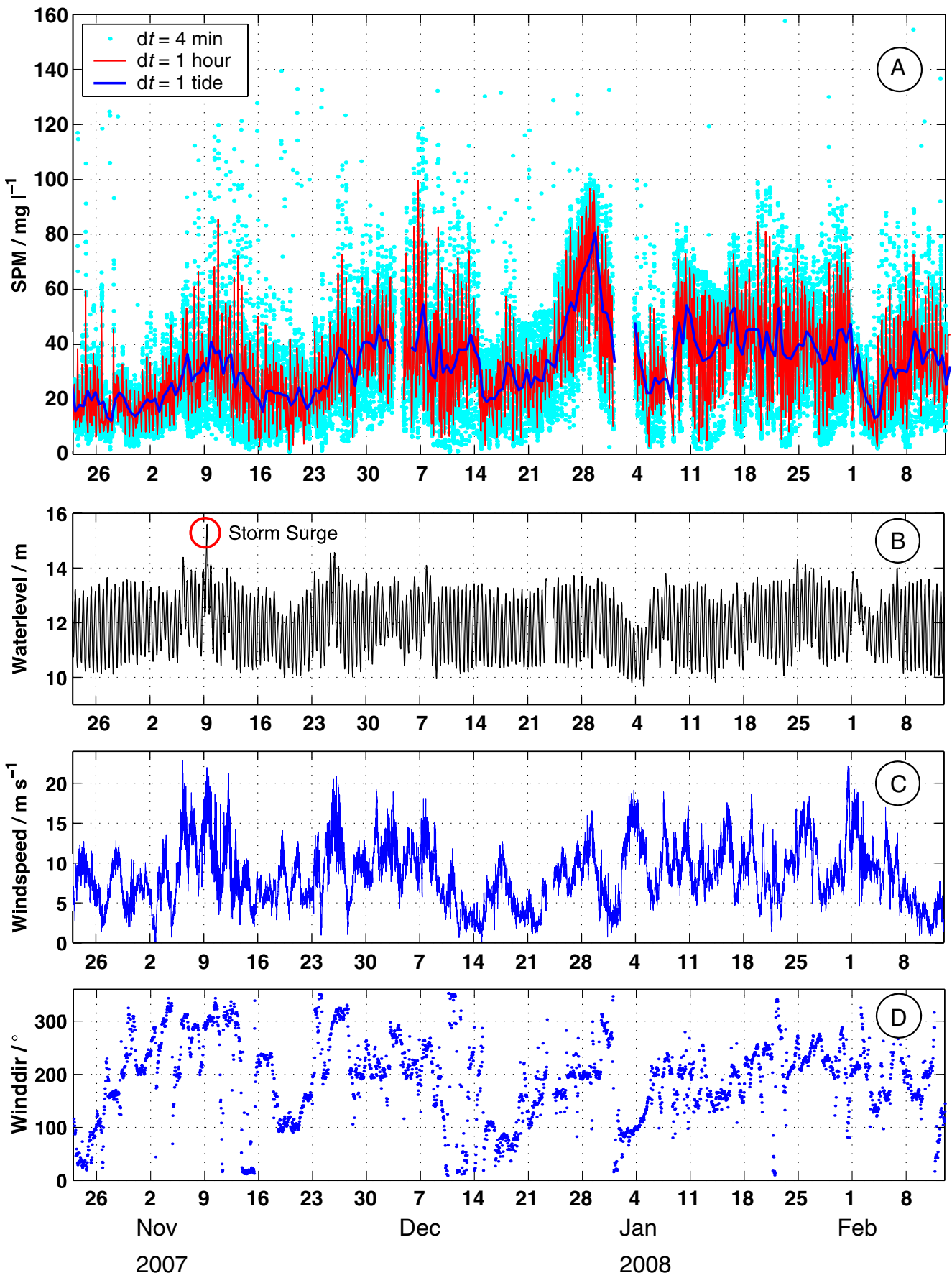

Fig. 12 SPM measured with LISST by vertical profiling and gridded to 0.75 m intervals (October 2007). Data are related to the seafloor. *HW*: high water, *LW*: low water

(Figs. 11 and 12). For reasons of clarity, the plots were related to the sea floor. The data from both methods correspond well. The highest SPM concentrations were found close to the sea floor about 1 h after the current maxima.
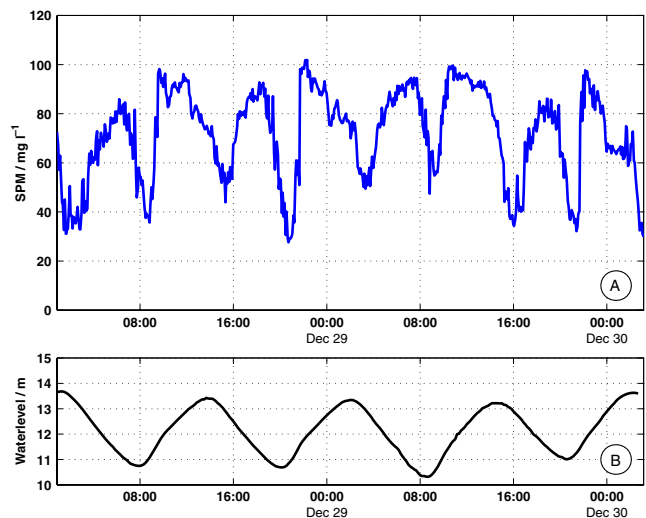
3.2 Time Series Station

In order to test the suitability of multispectral transmission measurements for estimating in situ SPM, the Trios-MST has been mounted to the Time Series Station since autumn 2006. During the initial test period, some problems occurred, such as a severe corrosion of metallic instrument parts. The device was therefore reconstructed using a titanium housing.

The MST-derived SPM data (Fig. 13) were calculated using the algorithm as described in Section 2.1.1. In this calculation, the *Chl a* values were set to zero. SPM values were derived by subtracting Gelbstoff values from the measured attenuation coefficient. The resulting data were converted to absolute values using data obtained by the filter method aboard *FK Senckenberg* in October 2007.

As can be clearly seen, SPM concentrations varied considerably (range 0.2 to 160 mg l^{-1}) over the study period (Fig. 13). The instantaneous measurements (light blue dots) were conducted every 4 min.
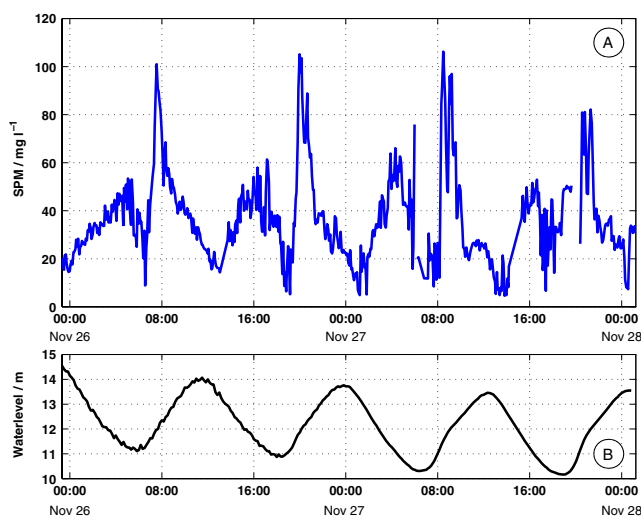
Fig. 14 Trios-MST-derived SPM concentrations (detection interval 4 min) **a** and water level **b** at the Wadden Sea Time Series Station from 26 to 28 November 2007

Fig. 15 Trios-MST-derived SPM concentrations (detection interval 4 min) **a** and water level **b** at the Wadden Sea Time Series Station from 28 to 30 December 2007

This enabled the detection of fluctuations on a small time scale. Data were also averaged for periods of 1 h (red line) and one tidal cycle (blue line): The results show that special events such as the storm surge on 9 November 2007 (winter storm "Tilo" with wind speeds up to 10 Bft, see Fig. 13b and c) were followed by a strong increase of SPM concentrations. A closer look at the data reveals that SPM fluctuations are mainly influenced by tidal currents (Figs. 14 and 15). As the tide rises, SPM concentrations increase sharply to a maximum value shortly after current maximum in the middle of the flooding period. The lowest SPM values occur with a time lag of approximately 1 h after slack water.

This signal, however, varies depending on wind direction (Fig. 13d). From 26 to 28 November, wind speed and direction was similar to storm Tilo, and the tidal means of SPM concentrations range in the same order of magnitude. On both occasions, the intratidal variability was high (Fig. 14). Opposite to that, from 28 to 30 December, intratidal SPM dynamics were lower (Fig. 15) while the tidal means of SPM concentrations were much higher (Fig. 13a), even though wind speeds did not exceed 8 Bft. Here, southwesterly winds were prevailing.

4 Discussion

4.1 Comparison of methods

The data presented in this study demonstrate the suitability of MST measurements for obtaining long-term

SPM data in coastal turbid waters. In both laboratory and ship-based observations, MST data correlate well with data obtained by the filter method. The results also demonstrate the wide range of SPM concentrations (0.2 to 160 mg l^{-1}) occurring in this highly variable system. The MST is particularly suited for such conditions since its optical path length can be adjusted to varying concentrations. Even though this can be remotely controlled, the adjustment itself has to be done manually and is therefore checked only once a day during workdays. Thus, this procedure cannot account for fluctuations occurring on time scales of minutes or hours. In the future, an optimised optical path length could be automatically adjusted with a new sensor control software which includes this feature.

The path lengths (20 to 40 mm) that are commonly used for the conditions at the time series station are not suited for concentrations below <5 mg l^{-1}. This was also confirmed during the laboratory measurements (Fig. 5). However, this problem is overcome since such low concentrations rarely occur in the Wadden Sea area (Lane et al. 2000; Gemein et al. 2006; Lunau et al. 2006; Dellwig et al. 2007).

Another advantage of the MST is the instrument's capability for in situ calibration by remote control, as described in Section 2.1.1. This allows for continuous checking of possible biofouling and instrument failure. Thus, maintenance visits to the time series station, which are costly and time consuming, can be reduced to a minimum.

In the Wadden Sea, particles with a radius smaller than approximately 30 μm are indeed distributed according to Junge (Fig. 9). This view is supported by the fact that both LISST and MST data result in similar values. This study result provides valuable insight for sediment modeling.

Another promising result is that both MST- and LISST-derived SPM concentrations correspond well. The naturally occurring fluctuations in SPM concentrations as measured aboard FK Senckenberg in October 2007 were equally detected by both instrument types (Fig. 10). However, due to the fundamentally different measuring principles, the results also deviate from each other. For example, at the beginning of the measuring period on October 17 (Figs. 10, 11 and 12), LISST values were higher than ME-MST values. Such differences may be caused by variations in the size distribution of particles (Fig. 8): When particles with radii above 50 μm dominate, and when particles at these sizes are not distributed according to Junge, the MST might underestimate SPM concentrations.

As for the LISST, on the one hand, there are known disadvantages of the method, such as multiple scat-tering at turbidities higher than 20 m^{-1} (Agrawal and Pottsmith 2000). This did not affect the LISST measurements in this study since turbidity was less than 16 m^{-1}. Nevertheless, higher turbidities do occur in the Wadden Sea as can be inferred from Figs. 13 and 6. On the other hand, the MST cannot measure absolute volume concentrations of different particle sizes, but merely the relative particle size distribution by means of the Junge coefficient and assuming a hyperbolic particle size distribution (Barth et al. 1997).

4.2 Time series data

This paper presents high-resolution, long-term SPM measurements obtained at the Wadden Sea Time Series Station. To our knowledge, such a data set has not been shown before. The data reveal the strong fluctuations of SPM concentrations in highly dynamic tidal inlets. In addition, special events, such as the storm surge on 9 November 2007, are captured. These data are valuable for estimating the impact of such events on sediment dynamics in the Wadden Sea. For instance, they can be used to validate model calculations Lettmann et al. (2009) and Wolff et al. (2009). However, the data also indicate that westerly to northwesterly winds or gales prevailing for a couple of days have about the same or even larger impact on SPM concentrations than a single storm surge, such as from 26 to 30 November 2007 and 5 to 7 December 2007 (Fig. 13). These conditions generate large surface waves, which break in front of the East Frisian Islands and resuspend substantial amounts of sediment in the water column (Lettmann et al. 2009). This view is also supported by Fig. 14: The most pronounced increase in SPM concentrations and maximum values occur during the flooding period.

The relationship between water level and current velocities at the study site is discussed in Reuter et al. (2009) and Bartholomä et al. (2009). In general, the slack water period during low tide is longer than that during high tide. Current maxima occur in the middle of each tide and the area is ebb-dominated (Stanev et al. 2003a, b). A closer look at the tidal cycles shown in Figs. 14 and 15 reveals the dependence of elevated SPM concentrations on current maxima at mid-tide. Previous studies performed at the same location also found this pattern (Lunau et al. 2006). Manual sampling with a lower sampling interval would most likely miss such maxima, as well as higher concentrations generated by sediment plumes (Winter et al. 2007). Tidal SPM maxima were, for example, also observed by Grabemann and Krause (2007) in the Weser Estuary. These authors

report a shift of concentration maxima during the tidal cycle from a landwards via a central to a seawards part of the estuary depending on river runoff. The pattern observed in our study corresponds well to the pattern observed in the central part of the Weser estuary.

The time series data also reveal high tidal means of SPM concentrations between Christmas and New Year's Eve in 2007 (Fig. 13a). During this period, southwesterly winds prevailed for several days (Fig. 13c and d). Due to these conditions, the SPM remained resuspended in the water column and was transported during ebb tide from the back-barrier flats far into the open North Sea. With the next flood, this material was carried back through the tidal inlets. This process is reflected in Fig. 15, which shows less intratidal variation in SPM dynamics than during the high-energy period with northwesterly winds (Fig. 14). Such SPM plumes reaching far into the open sea during southwesterly winds have been observed before by means of satellite images (Gemein et al. 2006).

The periods discussed above indicate that longer lasting winds may have a larger impact on SPM dynamics in the study area than a single storm surge. Bartholdy and Aagaard (2001) also conclude that one extreme episodic storm can be of less importance for annual variations in sediment deposition in the Danish Wadden Sea than more frequent gales.

Spring and neap tides are often discussed as important factors influencing sediment dynamics in the Wadden Sea (Bartholomä et al. 2009). However, during the study period reported here, no distinctive spring and neap tides could be observed. The variations in water level and SPM concentrations seemed to be mainly driven by wind and waves.

5 Conclusions

This study demonstrated that the MST-derived SPM data correspond well with SPM data derived from standard methods. The instrument has been proven valuable for in situ long-term measurements. The data set provides a detailed view on SPM dynamics during winter months, in particular, extreme events such as storm surges. Such high temporal resolution over periods of weeks to months cannot be achieved by either shipboard or satellite observations. In the future, the deployment of a second MST close to the seafloor could provide important information on bottom sediment dynamics.

Data obtained at the Wadden Sea Time Series Station are already successfully used for model validation

(Staneva et al. 2009; Burchard et al. 2008; Lettmann et al. 2009). The results from highly resolved SPM measurements will serve as a validation tool for existing and future models and provide background data for estimating the influence of climate change on coastal sediment dynamics, such as in the study by Stanev et al. (2006).

References

Agrawal Y, Pottsmith H (2000) Instruments for particle size and settling velocity observations in sediment transport. Mar Geol 168:89–114

Agrawal YC (2005) The optical volume scattering function: temporal and vertical variability in the water column off the New Jersey coast. Limnol Oceanogr 50(5):1787–1794

Agrawal YC, Whitemire A, Mikkelsen OA, Pottsmith HC (2008) Light scattering by random shaped particle and consequences on measuring suspended sediments by laser diffraction. J Geophys Res 113(C04023):1–11

Astoreca R, Ruddick K, Rousseau V, Mol BV, Parent JY, Lancelot C (2006) Variability of the inherent and apparent optical properties in a highly turbid coastal area: impact on the calibration of remote sensing algorithms. EARSeL eProc 5(1):1–17

Austin R, Petzold T (1977) Considerations in the design and evaluation of oceanographic transmissometers. In: Tyler JE (ed) Light in the sea. Dowden, Hutchinson and Ross, Stroudsburg, pp 104–120

Barth H, Grisard K, Holtsch K, Reuter R, Stute U (1997) Polychromatic transmissometer for in situ measurements of suspended particles and gelbstoff in water. Atmos-Ocean 36(30):7919–7928

Barth H, Reuter R, Schröder M (2000) Measurement and simulation of substance specific contributions of phytoplankton, gelbstoff, and mineral particles to the underwater light field in coastal waters. EARSeL eProc (1):165–174

Bartholdy J, Aagaard T (2001) Storm surge effects on a back-barrier tidal flat of the Danish Wadden Sea. Geo Mar Lett 20:133–141

Bartholomä A, Kubicki A, Badewien TH, Flemming B (2009) Suspended sediment transport in the German Wadden Sea—seasonal variations and extreme events. Ocean Dyn (in press)

Bricaud A, Morel A, Prieur L (1981) Absorption by dissolved organic matter of the sea (yellow substance) in the UV visible domains. Limnol Oceanogr 26(1):43–53

Burchard H, Flöser G, Staneva J, Badewien TH, Riethmüller R (2008) Impact of density gradients on net sediment transport into the Wadden Sea. J Phys Oceanogr 38:566–587

Dellwig O, Beck M, Lemke A, Lunau M, Kolditz K, Schnetger B, Brumsack HJ (2007) Non-conservative behaviour of molyb-

denum in coastal waters: coupling geochemical, biological, and sedimentological processes. Geochim Cosmochim Acta 71(11):2745–2761

Diehl P, Haardt H (1980) Measurement of the spectral attenuation to support biological research in a "plankton tube" experiment. Oceanol Acta 3(1):89–96

Gemein N, Stanev E, Brink-Spalink G, Wolff JO, Reuter R (2006) Patterns of suspended matter in the East Frisian Wadden Sea: comparison of numerical simulations with MERIS observations. EARSeL eProc 2(5):180–198

Grabemann I, Krause G (2007) On different time scales of suspended matter dynamics in the Weser estuary. Estuaries 218:1–16

Lane A, Riethmüller R, Herbers D, Rybaczok P, Günther H, Baumert H (2000) Observational data sets for model development. Coast Eng 41:125–153

Lettmann K, Wolff JO, Badewien TH (2009) Impact of wind generated surface gravity waves and extreme events on sediment dynamics of an intertidal flat system in the East Frisian Wadden Sea (southern North Sea, Germany). Ocean Dyn (in press)

Lumborg U, Pejrup M (2005) Modelling of cohesive sediment transport in a tidal lagoon an annual budget. Mar Geol 24(5):688–698

Lunau M, Lemke A, Dellwig O, Simon M (2006) Physical and biogeochemical controls of microaggregate dynamics in a tidally affected ecosystem. Limnol Oceanogr 51(2): 847–859

Mehrtens C, Badewien T, Reuter R (2009) Airborne digital imagery for suspended matter detection in the East Frisian Wadden Sea, Germany. EARSeL eProc (in press)

Puncken O, Badewien TH, Reuter R (2006) MOSES (measuring system for the oberservation of sea surfaces): Lagrangian drift experiments in the East Frisian Wadden Sea. In: Marcal A (ed) Global developments in environmental earth observation from space. Millpress, Rotterdam, pp 697–706

Reuter R (1980) Characterization of marine particle suspensions by light scattering II. Experimental results. Oceanol Acta 3(3):325–332

Reuter R, Badewien TH, Bartholomä A, Braun A, Lübben A, Rullkötter J (2009) A hydrographic time-series station in the Wadden Sea (southern North Sea. Ocean Dyn (in press)

Santamarina CP, Flemming B (2000) Quantifying the concentration and flux of suspended particulate matter through a tidal inlet of the East Frisian Wadden Sea by acoustic doppler current profiling. In: Flemming BWMTD, Liebezeit G (eds) Muddy coast dynamics and resource management. Elsevier Science, Amsterdam, pp 39–52

Stanev EV, Flöser G, Wolff JO (2003a) Dynamical control on water exchanges between tidal basins and the open ocean. A case study for the East Frisian Wadden Sea. Ocean Dyn 53:146–165

Stanev EV, Wolff JO, Brink-Spalink G (2006) On the sensitivity of the sedimentary system in the East Frisian Wadden Sea to sea-level rise and wave-induced bed shear stress. Ocean Dyn 56:266–283

Stanev EV, Wolff JO, Burchard H, Bolding K, Flöser G (2003b) On the circulation in the East Frisian Wadden Sea: numerical modelling and data analysis. Ocean Dyn 53:27–51

Staneva J, Stanev E, Wolff JO, Badewien TH, Reuter R, Flemming B, Bartholomä A, Bolding K (2009) Dynamics and sediment dynamics in the German Bight. A focus on observations and numerical modelling in the East Frisian Wadden Sea. Continental Shelf Res 29(1):302–319

Winter C, Becker M, Ernstsen VB, Hebbeln D, Port A, Bartholomä A, Flemming B, Lunau M (2007) In-situ observation of aggregate dynamics in a tidal channel using acoustics, laser diffraction and optics. J Coast Res SI(50): 1173–1177

Wolff JO, Reuter R et al (2009) High resolution modelling of hydro- and sediment dynamics in the East Frisian Wadden Sea (southern North Sea). Ocean Dyn (in press)